

Nuclear structure and decay properties of even-even nuclei in $Z = 70 - 80$ drip-line region

S. Mahapatro^{1*}, C. Lahiri^{2*†}, Bharat Kumar², R. N. Mishra¹ and S. K. Patra²

¹Department of Physics, Ravenshaw University, Cuttack-753003, India.

²Institute of Physics, Sachivalaya Marg, Bhubaneswar 751005, India.

November 6, 2018

Abstract

We study nuclear structure properties for various isotopes of Ytterbium (Yb), Hafnium(Hf), Tungsten(W), Osmium(Os), Platinum(Pt) and Mercury(Hg) in $Z = 70 - 80$ drip-line region starting from $N = 80$ to $N = 170$ within the formalism of relativistic mean field (RMF) theory. The pairing correlation is taken care by using BCS approach. We compared our results with Finite Range Droplet Model(FRDM) and experimental data and found that the calculated results are in good agreement. Neutron shell closure are obtained at $N = 82$ and 126 in this region. We have also studied probable decay mechanisms of these elements.

PACS Number(s): 21.10.Dr,21.10.Pc,21.10.Tg,23.40.-s,23.60.+e

1 Introduction

Recent developments of Radioactive Ion Beam (RIB) facilities has encouraged various experimental as well as theoretical developments for nuclei far from the β stability line. Physics of nuclear structure and decay mechanism in neutron rich nuclei is a very popular field of study in present days [1, 2]. Recently the study of deformed nuclear shapes is also a very interesting topic and a number of excellent review articles exist [3, 4, 5, 6] in this context. In literature, after the early calculations, which have predicted the existence of the superdeformed shape (see Ref.[2] for the review), its first experimental discovery took place in 1985 [7]. Till then numerous groups have developed sophisticated techniques to perform calculations allowing the description of rotational bands for very elongated shapes. The phenomenon of superdeformation constitutes a spectacular manifestation of the mean-field properties of nuclei.

*Email:narayan@iopb.res.in

†clahiri@iopb.res.in

The change of shape of nuclei and other properties of nuclear structure with neutron number has attracted much theoretical and experimental attention for many years [8, 9, 10, 11, 12]. The conditions needed for the observation of shapes coexisting in such nuclei have been a matter of challenge and theoretically calculated by Patra and Panda [13] in 1993. The change of shapes of Pt isotopes was studied by Sharma and Ring [14]. The shapes of nuclei such as Os and Pt have also been studied by using the Hartree-Fock Bogoliubov (HFB) formalism within the non-relativistic framework [8]. Recently B. Kumar *et al.* [15] studied the shape co-existence in Zr isotopes.

The nuclei with $Z = 70 - 80$ consists of both Rare Earth Metals(Yb) as well as the Transition metals(Hf, W, Os, Pt, Hg). They manifest a lot of interesting phenomena like shape co-existence, change of shape in an isotopic chain etc [16, 17]. In this region of the atomic number, variety of shapes such as prolate, oblate and spherical configuration of nuclei appears in ground state[18].

Many theoretical as well as experimental papers have focused their interest on the shape transition [19], shape isomerism and the observation of superdeformed bands [20] in neutron-deficient Hg isotopes.

The aim of this manuscript is to explore the neutron rich side of the concerned mass region with RMF formalism. Mainly the structure informations like deformation, two neutron separation energy, single particle energy levels etc. have been extracted using NL3 force parameter.

Further, α decay has been remained a very powerful tool to study the nuclear structure since its discovery by Becquerel in 1896. We also find other exotic decay modes like β decay, spontaneous fission, cluster-decay etc. Therefore, it will be interesting to see the preferred decay modes of these neutron-rich even-even nuclei.

The paper is organized as follows. In section 2, we have given a brief outline about the relativistic mean field (RMF) formalism. The effects of pairing for open shell nuclei, included in our calculations, are also discussed in this section. Our results are discussed in section 3. The reaction Q values for α and β decay and their corresponding half lives are given in section 4. A concluding remark is given in section 5.

2 Theoretical Framework for Relativistic Mean Field Model

The relativistic mean field (RMF) model [21, 22, 23, 24, 25, 26, 27, 28] is a well applied technique in recent years and have been applied to finite nuclei and infinite nuclear matter. In the present work, we have taken the RMF Lagrangian [21] with NL3 parameter set [29] in our study. This force parameter set is successful in both β -stable and drip-line nuclei. The Lagrangian contained the term of interaction between meson and nucleon and also self-interaction of isoscalar-scalar *sigma* meson. The other mesons are isoscalar-vector *omega* and isovector vector *rho* mesons. The photon field A_μ is included to take care

of Coulombic interaction of protons. The pairing correlation is taken care by using BCS approach [21]. We start with the relativistic Lagrangian density for a nucleon-meson many-body system,

$$\begin{aligned}
\mathcal{L} = & \bar{\psi}_i \{ i\gamma^\mu \partial_\mu - M \} \psi_i + \frac{1}{2} \partial^\mu \sigma \partial_\mu \sigma - \frac{1}{2} m_\sigma^2 \sigma^2 \\
& - \frac{1}{3} g_2 \sigma^3 - \frac{1}{4} g_3 \sigma^4 - g_s \bar{\psi}_i \psi_i \sigma - \frac{1}{4} \Omega^{\mu\nu} \Omega_{\mu\nu} \\
& + \frac{1}{2} m_\omega^2 V^\mu V_\mu + \frac{1}{4} c_3 (V_\mu V^\mu)^2 - g_\omega \bar{\psi}_i \gamma^\mu \psi_i V_\mu \\
& - \frac{1}{4} \vec{B}^{\mu\nu} \cdot \vec{B}_{\mu\nu} + \frac{1}{2} m_\rho^2 \vec{R}^\mu \cdot \vec{R}_\mu - g_\rho \bar{\psi}_i \gamma^\mu \vec{\tau} \psi_i \cdot \vec{R}^\mu \\
& - \frac{1}{4} F^{\mu\nu} F_{\mu\nu} - e \bar{\psi}_i \gamma^\mu \frac{(1 - \tau_{3i})}{2} \psi_i A_\mu.
\end{aligned} \tag{1}$$

Here sigma meson field is denoted by σ , omega meson field by V_μ and rho meson field is denoted by ρ_μ . In the equations, A^μ denotes the electromagnetic field, which couples to the protons. ψ are the Dirac spinors for the nucleons, whose third components of isospin is τ_3 and $g_s, g_2, g_3, g_\omega, c_3, g_\rho$ are the coupling constants. A definite set of coupled equations are obtained from the above Lagrangian and solved self-consistently in an axially deformed harmonic oscillator basis. The total energy of the system is given by the expression,

$$E_{total} = E_{part} + E_\sigma + E_\omega + E_\rho + E_c + E_{pair} + E_{c.m.}, \tag{2}$$

where E_{part} is the sum of the single-particle energies of the nucleons and $E_\sigma, E_\omega, E_\rho, E_c, E_{pair}$ are the contributions of the meson field, the coulomb field and the pairing energy respectively. The center of mass (c.m.) motion energy correction is estimated by the harmonic oscillator formula $E_{c.m.} = \frac{3}{4} (41A^{-1/3})$ MeV, where A is the mass number of the nucleus. The total quadrupole deformation parameter β_2 and hexadecupole parameter β_4 of the nucleus can be obtained from the quadrupole moment Q and hexadecupole moment H , respectively using the relations

$$\beta_2 = \sqrt{\frac{5\pi}{9}} \frac{Q}{AR^2} \quad \& \quad \beta_4 = \frac{4\pi}{3} \frac{H}{AR^4}, \tag{3}$$

where R is the nuclear radius. The root mean square (rms) matter radius is given as

$$\langle r_m^2 \rangle = \frac{1}{A} \int \rho(r_\perp, z) \cdot r^2 d\tau \tag{4}$$

Here $\rho(r_\perp, z)$ is the deformed density. The total binding energy and other observables are also obtained by using the standard relations, given in [21, 22].

2.1 Pairing Correlations in RMF formalism

Pairing correlation is playing very crucial role in open shell nuclei. In our calculation we are using the Bardeen-Cooper-Schrieffer (BCS) pairing for determining

the bulk properties like binding energy (BE), quadrupole deformation parameter and nuclear radii. The pairing energy can be given as:

$$E_{pair} = -G \left[\sum_{i>0} u_i v_i \right]^2, \quad (5)$$

where G is pairing force constant and v_i^2 , $u_i^2 = 1 - v_i^2$ are the occupation probabilities respectively [30, 21, 31]. The simple form of BCS equation can be derived from the variational method with respect to the occupation number v_i^2 and is given by:

$$2\epsilon_i u_i v_i - \Delta(u_i^2 - v_i^2) = 0, \quad (6)$$

using $\Delta = G \sum_{i>0} u_i v_i$.

The occupation number is defined as:

$$n_i = v_i^2 = \frac{1}{2} \left[1 - \frac{\epsilon_i - \lambda}{\sqrt{(\epsilon_i - \lambda)^2 + \Delta^2}} \right]. \quad (7)$$

In this calculation we are dealing with the constant gap formalism for proton and neutron in a region far from beta stability line. These constant gap equation for proton and neutron is taken from Ref. [32, 33] which is given as:

$$\Delta_p = R B_s e^{sI - tI^2} / Z^{1/3} \quad (8)$$

and

$$\Delta_n = R B_s e^{-sI - tI^2} / A^{1/3}, \quad (9)$$

with $R=5.72$, $s=0.118$, $t=8.12$, $B_s=1$, and $I = (N - Z)/(N + Z)$. In our present calculation, we have taken the constant pairing gap for all states $|\alpha\rangle = |nljm\rangle$ near the Fermi surface for the sake of simplicity. Similar approach was used in the references [34, 35, 36].

As we know, if we go near the neutron drip line, then coupling to the continuum become important [37, 38, 39, 40]. In this case the Relativistic Hartree-Bogoliubov (RHB) approach [41, 42] has been proved to be a more accurate formalism for this region. However in case of RMF-BCS formalism also, the pairing constants along with NL3 parameters are adjusted so that it can reproduce the bulk properties of a nucleus near the drip line region. For example, in Fig. 1 the total binding energy/nucleon (BE/A) for Hg isotopes from our calculation are compared with available NL3-RHB data [43] along with existing FRDM [44] and experimental results [45]. The other components of our present calculation like the selection of basis space is described in the next section. It is evident from the figure that the binding energy from our calculation is in a nice agreement with FRDM and experimental results in neutron rich region. Further, our present result agrees acceptably well with the available RHB data. By using BCS pairing correlation model, it has been shown earlier by different groups [46, 47, 48, 49, 50] that the results from relativistic mean field BCS (RMF-BCS) approach is almost similar with the RHB formalism. However due

to the lack of NL3-RHB data in neutron rich region for the concerned isotopes, we are unable to compare their individual merits, but the above figure and references suggest that the present formalism can be extended in neutron rich region.

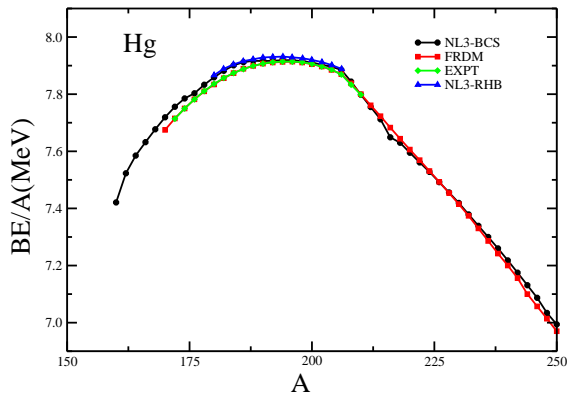


Figure 1: (Color online) The binding energy per particle (BE/A) obtained from RMF(NL3-BCS) (circle) compared with RHB (triangle) [43] FRDM (square) [44] and experimental (diamond) [45] data for Hg isotopes.

2.2 Selection of Basis Space

In order to choose the proper basis, we calculate the physical observables like binding energy, root mean square(rms) radii and quadrupole deformation parameter(β_2). To select optimal values for N_F and N_B , we select ^{220}Yb and ^{230}Hg as test case and increase the basis quanta from 8 to 20 step by step in Fig. 2. We find that these physical observables varies with changing the bosonic and fermionic oscillator quanta $N_F=N_B=8$ to 12 but become almost constant after $N_F=N_B=14$. But our calculation is extended far beyond the stability line which demands a comparatively large basis space for calculation. Therefore for greater accuracy, we have chosen $N_F=N_B=20$ for all the calculations. Similar types of calculation are found in Refs.[51, 52, 15, 21, 53].

3 Calculations and Results

Relativistic mean field model have given very good result in β - stable nuclei of the nuclear landscape. In this work we are analyzing the exotic neutron drip line nuclei by using RMF model with well known NL3 [29] parameter set. In 1999, Lalazassis *et al.* [18] analyzed ground-state properties of 1315 even-even

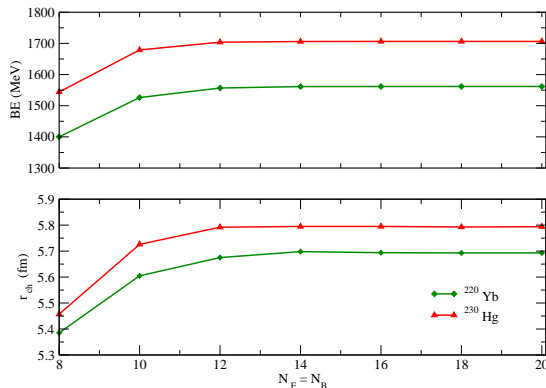


Figure 2: (Color online) The variation of calculated binding energy (BE), charge radii (r_c) with increasing number of Bosonic and Fermionic basis.

nuclei with Z between 10 and 98 and calculated total binding energy, radius and deformations using similar formalism mostly near the stability region. In the present manuscript, we have extended the RMF-BCS formalism near the neutron drip line for even-even nuclei in $Z = 70 - 80$ region. In Tables 1-6, the ground state binding energy, neutron, proton, charge and r.m.s. radius, quadrupole and hexadecupole parameter of the above isotopes are compared with FRDM [44, 54] and experimental data [45, 55, 56]. In the upcoming subsections our results are described in detail.

3.1 Quadrupole Deformation

The Quadrupole deformation parameter β_2 for the ground state for even-even nuclei in $Z = 70 - 80$ region are determined within the RMF-BCS formalism near the neutron drip-line as an extension of existing data[18]. The parameter β_2 is directly connected to the shape of the nucleus. The ground state quadrupole deformation parameter β_2 is plotted in Fig. 3. We have compared our RMF results with FRDM [54] results.

In case of Yb isotopes in Fig. 3, RMF β_2 data coincides with FRDM [54] values for almost all the mass numbers. In lower mass regions, Yb isotopes are nearly spherical ($A = 150$). It changes to oblate at $A = 155$. The prolate stage exists from $A = 160 - 190$. At $A = 190 - 200$, it changes from spherical to oblate. At $A = 200 - 230$ again it changes to prolate state. In lower and higher mass region, maximum isotopes are prolate in shape. In the middle region, these changes to oblate shape. Therefore one can say that, in Yb isotopes, at $A = 155$ and 190 , there is a shape transition from oblate to highly prolate. FRDM also shows the same trend in shapes. The same trend is found in other

isotopes except mercury (Hg). Mercury shows prolate shape at $A = 170 - 190$ whereas FRDM shows oblate shape in the same region.

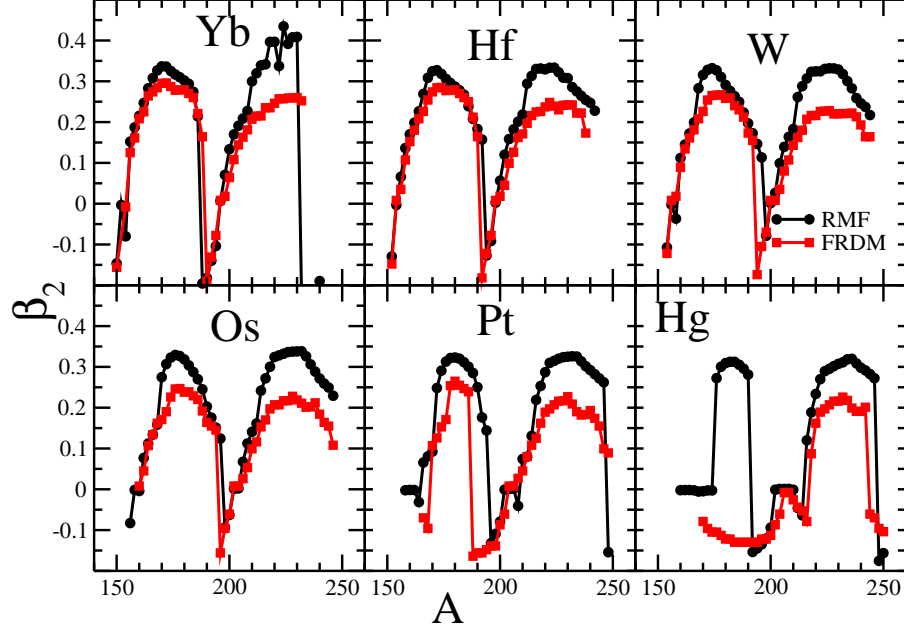


Figure 3: (Color online) The quadrupole moment deformation parameter β_2 obtained from RMF(NL3)(circle) compared with the Finite Range Droplet Model(FRDM) (square) [54] results for different isotopes of Yb, Hf, W, Os, Pt and Hg in $Z = 70 - 80$ drip-line region.

3.2 Two-neutron separation energy

The two-neutron separation energy $S_{2n}(N,Z) = BE(N, Z) - BE(N-2, Z)$ is shown in Fig. 4 for Yb, Hf, W, Os, Pt and Hg isotopes. The S_{2n} values calculated from RMF, FRDM [44] and Experimental [45] results are compared in Fig. 4. We can predict the stability of these nuclei by S_{2n} energy. If S_{2n} is large, it means nuclei will be stable with two-neutron separation whereas the two neutron drip line for an isotopic chain can be identified as the nucleus having zero or slightly positive separation energy value. Therefore, it is evident from the figure that the two neutron drip line for the $Z = 70$ (Yb) isotope comes at $N = 166$, the same for $Z = 72, 74, 76$ isotopes is approximately at $N = 170$. In case of $Z = 80$ (Hg),

the two neutron drip line arrives at the neutron number $N = 168$. Furthermore, in all cases, the S_{2n} values decrease gradually with increase in neutron number. There is a kink appeared at neutron magic number $N = 126$ in every cases. In order to visualize this scenario with a bit clarity, in the next subsection, we defined differential variation of two-neutron separation energy given in Fig. 5.

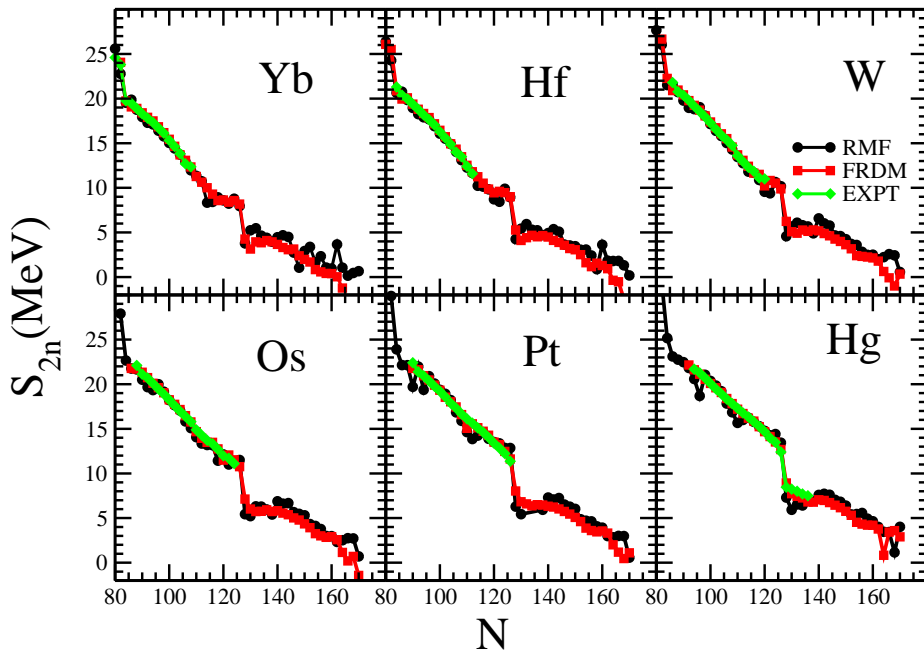


Figure 4: (Color online) Two-neutron separation energy S_{2n} (RMF)(circle) is compared with FRDM (square) and experimental results (diamond) for different isotopes of $Z = 70 - 80$ region.

3.3 Differential variation of two-neutron separation energy

The differential variation of the two-neutron separation energy S_{2n} with respect to the neutron number(N), i.e., $dS_{2n}(Z, N)$ is defined as:

$$dS_{2n}(Z, N) = \frac{S_{2n}(Z, N + 2) - S_{2n}(Z, N)}{2}. \quad (10)$$

The $dS_{2n}(Z, N)$ is important factor to find the rate of change of separation

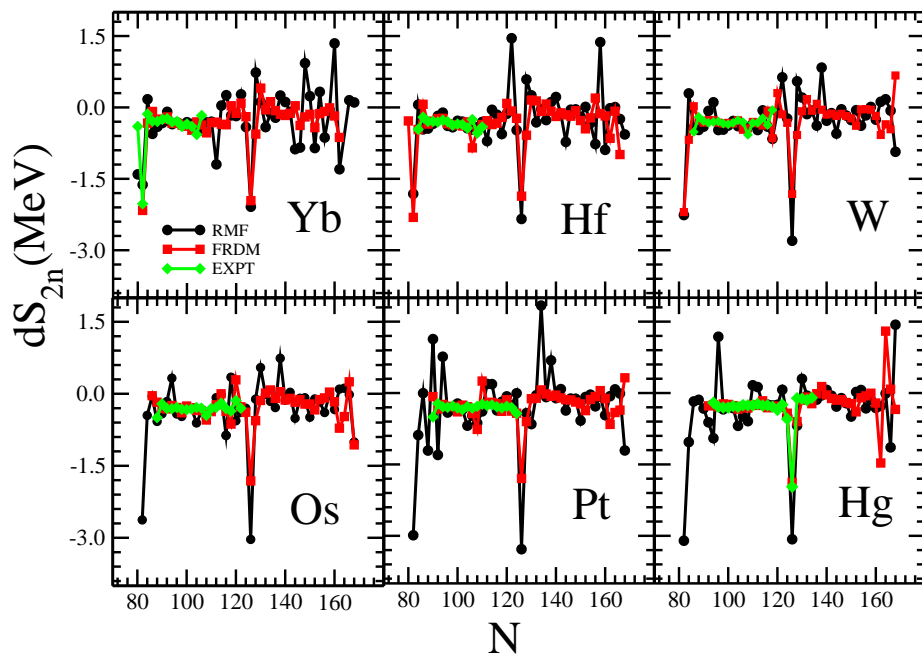


Figure 5: (Color online) The differential variation of two-neutron separation energy dS_{2n} (RMF)(circle) is compared with FRDM (square) and experimental results (diamond) for different isotopes of $Z = 70 - 80$ region.

energy with respect to the neutron number in an isotopic chain. Here, we calculated the $dS_{2n}(Z, N)$ for NL3 parameters and compared it with FRDM and experimental results extracted from refs. [44] and [45] respectively. In general, the large, sharp, deep fall in the $dS_{2n}(Z, N)$ is observed for Yb, Hf, W, Os, Pt and Hg isotopes at $N=82$ and $N=126$ (Fig. 5). It shows the neutron shell closures at $N = 82$ and $N = 126$.

3.4 Single Particle energy levels

In Fig. 6 we plotted single particle energies for neutron levels near the Fermi surface for Hg isotopes ($Z = 80$) at neutron shell closures ($N = 82$ & 126). We have used deformed configuration to calculate these levels. From Table 6, it is evident that ^{162}Hg and ^{206}Hg are nearly spherical and therefore the single particle levels are almost identical to that of the spherical configuration. For example, in ^{162}Hg , the level $g_{7/2}$ actually consists of four overlapped energy

Single particle energy levels for Hg isotopes (near Fermi surface)

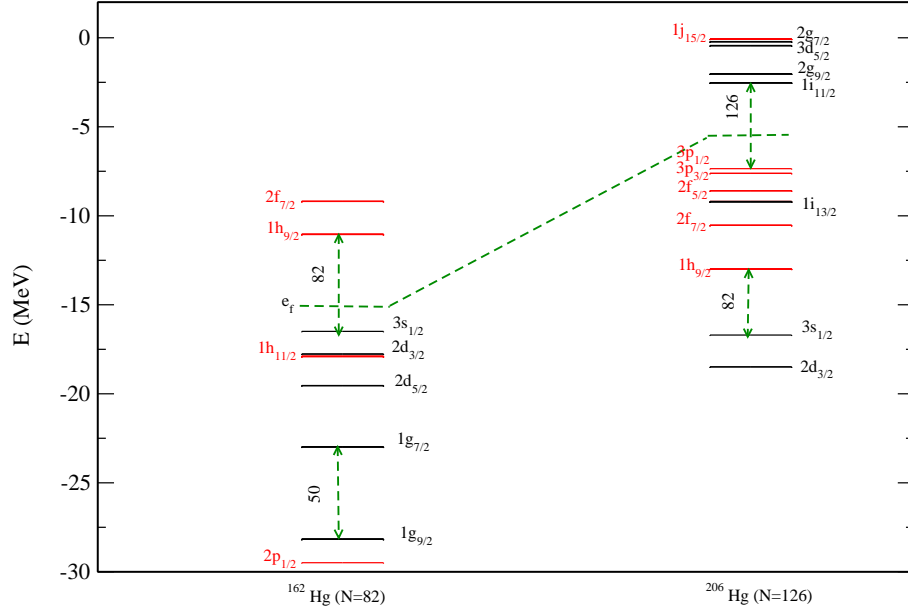


Figure 6: (Color online) The single particle energy levels for ^{162}Hg and ^{206}Hg isotopes from RMF model with NL3 parameter set. The dashed-line indicate the fermi surface e_f .

states having spins $7/2^+$, $5/2^+$, $3/2^+$ & $1/2^+$. In both cases, we found some large gaps at $N = 50, 82, 126$ shell closures. Here, the green dotted line shows the approximate fermi level. In case of Yb, Hf, W, Os and Pt also the gaps are visible at magic shell closures. However, they are not depicted in this manuscript.

4 Decay Modes

In this section we discuss probable decay modes of these neutron-rich nuclei.

4.1 Alpha decay half life

The Q_α energy is obtained from the relation [57]: $Q_\alpha(N, Z) = BE(N, Z) - BE(N - 2, Z - 2) - BE(2, 2)$. Here, $BE(N, Z)$ is the binding energy of the parent nucleus with neutron number N and proton number Z , $BE(2, 2)$ is the

binding energy of the α -particle (${}^4\text{He}$), i.e., 28.296 MeV, and $BE(N-2, Z-2)$ is the binding energy of the daughter nucleus after the emission of an α -particle.

The expression for the α -decay half life from Viola and Seaborg [58] is given by:

$$\log_{10}T_{1/2}^{\alpha}(s) = \frac{aZ - b}{\sqrt{Q_{\alpha}}} - (cZ + d) + h_{log}, \quad (11)$$

with Z as the number of proton for the parent nucleus and the constants a , b , c and d , are from Sobiczewski et al. [59]. The value of these constants are $a = 1.66175$, $b = 8.5166$, $c = 0.20228$, $d = 33.9069$ and the quantity h_{log} accounts for the hindrances associated with the odd nucleon as,

$$\begin{aligned} h_{log} &= 0 \text{ for } Z \text{ even and } N \text{ even} \\ &= 0.772 \text{ for } Z \text{ odd and } N \text{ even} \\ &= 1.066 \text{ for } Z \text{ even and } N \text{ odd} \\ &= 1.114 \text{ for } Z \text{ odd and } N \text{ odd.} \end{aligned} \quad (12)$$

We evaluate the BE by using RMF formalism and from these, we estimated the Q_{α} for all the isotopes of $Z = 70 - 80$ region. We have calculated the half-life time $T_{1/2}^{\alpha}$ by using the above formulae. The comparison of Q_{α} and $T_{1/2}^{\alpha}$ are shown in Fig. 7 and Fig. 8 respectively. From Fig. 8, it is evident that the alpha decay half life goes on increasing with large neutron numbers and follows similar trend for RMF, FRDM and experimental cases. In another word, we can say that, these neutron rich nuclei hardly exhibit α -decay and therefore the concerned decay channel is almost forbidden in this region.

In order to check the the usual decay mechanism of these neutron-rich samples, in the next subsection we studied the β decay half-life.

4.2 Beta decay half life

As discussed in the previous subsection, we expect β decay to be the prominent mode in case of neutron-rich nuclei. In order to calculate β decay half life, we have used the empirical formula of Fiset and Nix[60]. However the formula holds good mainly for the superheavy region, but in this work we have checked its credibility in $Z = 70 - 80$ region. The formula for β decay half life is defined as:

$$T_{1/2}^{\beta} = (540 \times 10^5) \frac{m_e^5}{\rho_{d.s.}(W_{\beta}^6 - m_e^6)}. \quad (13)$$

In the expression, $Q_{\beta} = BE(Z+1, A) - BE(Z, A)$ is the β decay Q value for the sample (Z, A) which decays to the daughter $(Z+1, A)$ and $W_{\beta} = Q_{\beta} + m_e^2$. Here, $\rho_{d.s.}$ is the average density of states in the daughter nucleus ($e^{A/290}$ \times number of states within 1 MeV of ground state). The approach has been applied in Th and U isotopes[52] recently. It is important to note that all the daughter nuclei $(Z+1, A)$ involved in our calculation are odd- Z nuclei. In these cases, the time reversal symmetry gets violated in the mean field models[52, 61]. Therefore,

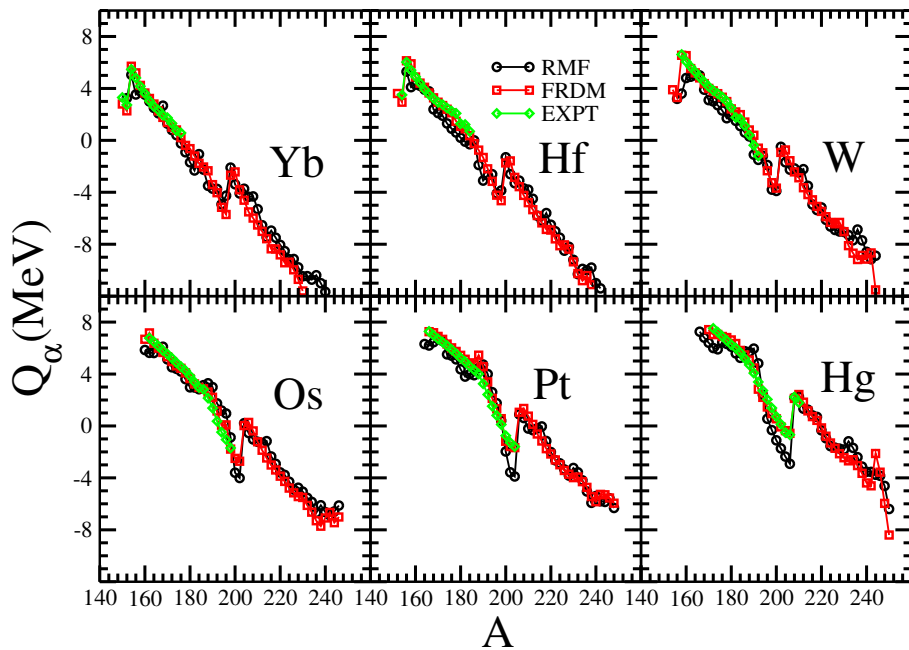


Figure 7: (Color online) The Q_α energy obtained from RMF(NL3)(circle) compared with the FRDM(square) and experimental(diamond) results for different isotopes of $Z = 70 - 80$ region.

to evaluate the binding energy of odd- Z nuclei, we used the Pauli blocking prescription [61] which restores the time-reversal symmetry. In Fig. 9 and Fig. 10 our results for Q_β and $T_{1/2}^\beta$ are displayed, respectively. For comparison, FRDM results are also given. One can see that RMF results almost follow the similar trend as that of FRDM results which confirms the applicability of the above formula[60] in $Z = 70 - 80$ mass region. Further, from Fig. 10 we can conclude that the decay of these nuclei mainly choose β decay as the prominent path.

5 Summary and Conclusion

We have calculated quadrupole deformation, hexadecupole deformation, two neutron separation energy and differential variation of two neutron separation energy for some neutron-rich even-even nuclei in $Z = 70 - 80$ region using RMF theory with pairing correlation from BCS approach (RMF-BCS). The results from S_{2n} and dS_{2n} confirm the neutron shell closure at $N = 82$ and 126 . As a further confirmatory test, the single particle energy levels for neutrons in isotopic chains are examined. We observed large gaps at $N = 82$ and 126 . We have also calculated half lives for α and β decay and seen that neutron-rich

Table 1: The RMF(NL3) results for binding energy BE (MeV), Neutron, Proton, Charge, Root mean square radii(fm), quadrupole deformation parameter β_2 and hexadecupole parameter β_4 for Yb isotopes compared with the Finite Range Droplet Model (FRDM) data [44, 54] and available experimental results [45, 55, 56].

Nucleus	RMF (NL3)							FRDM			Expt.		
	BE(R)	r_n	r_p	r_{ch}	r_{rms}	β_2	β_4	BE(F)	β_2	β_4	BE(Ex)	r_{ch}	β_2
¹⁵⁰ Yb	1198.1	5.05	5.06	5.12	5.06	-0.15	-0.01	1194.6	-0.16	0.00	1194.6		
¹⁵² Yb	1220.9	5.06	5.04	5.11	5.05	-0.00	0.00	1218.6	-0.00	0.00	1202.4	5.04	
¹⁵⁴ Yb	1240.4	5.11	5.06	5.12	5.09	-0.08	0.01	1238.4	-0.01	0.00	1206.0	5.09	
¹⁵⁶ Yb	1260.3	5.16	5.09	5.15	5.13	0.15	0.05	1257.4	0.13	0.03	1257.6	5.12	
¹⁵⁸ Yb	1279.1	5.20	5.11	5.18	5.16	0.19	0.06	1276.3	0.16	0.03	1276.5	5.15	0.19
¹⁶⁰ Yb	1297.0	5.25	5.14	5.2	5.20	0.22	0.06	1294.8	0.21	0.02	1294.8	5.18	0.23
¹⁶² Yb	1314.3	5.29	5.16	5.22	5.23	0.25	0.08	1312.7	0.23	0.02	1312.6	5.21	0.26
¹⁶⁴ Yb	1331.4	5.34	5.18	5.25	5.27	0.28	0.11	1330.2	0.26	0.01	1330.0	5.23	0.29
¹⁶⁶ Yb	1347.8	5.38	5.21	5.27	5.31	0.31	0.11	1347.0	0.27	0.00	1346.7	5.25	0.32
¹⁶⁸ Yb	1363.6	5.42	5.23	5.29	5.34	0.33	0.10	1363.2	0.28	0.01	1362.8	5.27	0.32
¹⁷⁰ Yb	1378.6	5.45	5.25	5.31	5.37	0.34	0.07	1378.7	0.30	-0.03	1378.1	5.29	0.33
¹⁷² Yb	1393.0	5.48	5.26	5.32	5.40	0.34	0.04	1393.3	0.30	-0.04	1392.8	5.30	0.33
¹⁷⁴ Yb	1406.7	5.51	5.27	5.32	5.42	0.33	0.02	1407.0	0.29	0.02	1406.6	5.31	0.32
¹⁷⁶ Yb	1419.7	5.54	5.29	5.35	5.44	0.32	-0.00	1420.1	0.28	-0.07	1419.3	5.32	0.31
¹⁷⁸ Yb	1431.6	5.57	5.30	5.36	5.46	0.31	-0.03	1432.4	0.28	-0.09	1431.6		
¹⁸⁰ Yb	1443.0	5.60	5.31	5.37	5.49	0.3	-0.06	1443.7	0.28	-0.10	1442.5		
¹⁸² Yb	1453.7	5.63	5.32	5.38	5.52	0.29	-0.07	1454.3	0.27	-0.11			
¹⁸⁴ Yb	1462.0	5.66	5.33	5.39	5.54	0.27	-0.08	1464.3	0.26	-0.13			
¹⁸⁶ Yb	1470.5	5.66	5.32	5.38	5.54	0.21	-0.06	1473.6	0.22	-0.12			
¹⁸⁸ Yb	1479.4	5.69	5.32	5.38	5.55	-0.20	-0.02	1482.2	0.16	-0.08			
¹⁹⁰ Yb	1488.0	5.71	5.33	5.39	5.57	-0.18	-0.01	1490.8	-0.19	-0.03			
¹⁹² Yb	1496.2	5.73	5.33	5.39	5.59	-0.14	-0.02	1499.2	-0.13	-0.03			
¹⁹⁴ Yb	1505.0	5.75	5.33	5.39	5.60	-0.10	-0.03	1507.8	-0.08	-0.04			
¹⁹⁶ Yb	1513.0	5.77	5.33	5.39	5.62	0.01	0.00	1516.0	0.01	0.00			
¹⁹⁸ Yb	1516.7	5.82	5.35	5.41	5.66	0.07	0.02	1520.2	0.02	0.00			
²⁰⁰ Yb	1522.0	5.86	5.38	5.44	5.70	0.13	0.08	1523.4	0.06	0.04			
²⁰² Yb	1527.4	5.91	5.41	5.47	5.74	0.17	0.10	1527.3	0.11	0.06			
²⁰⁴ Yb	1532.1	5.95	5.43	5.49	5.78	0.19	0.09	1531.2	0.14	0.07			
²⁰⁶ Yb	1536.5	5.99	5.46	5.51	5.81	0.21	0.08	1535.3	0.16	0.08			
²⁰⁸ Yb	1540.4	6.03	5.48	5.53	5.85	0.23	0.08	1539.2	0.18	0.09			
²¹⁰ Yb	1544.9	6.08	5.54	5.60	5.91	0.30	0.20	1542.9	0.21	-0.08			
²¹² Yb	1549.6	6.12	5.56	5.62	5.95	0.32	0.20	1546.2	0.22	0.07			
²¹⁴ Yb	1554.1	6.16	5.59	5.65	5.98	0.34	0.21	1549.3	0.22	0.06			
²¹⁶ Yb	1556.8	6.20	5.6	5.66	6.01	0.34	0.19	1552.4	0.24	0.05			
²¹⁸ Yb	1557.9	6.26	5.65	5.71	6.07	0.40	0.10	1554.8	0.24	0.03			
²²⁰ Yb	1560.8	6.29	5.67	5.72	6.10	0.40	0.08	1556.8	0.25	-0.01			
²²² Yb	1564.2	6.29	5.65	5.70	6.09	0.34	0.09	1558.5	0.26	-0.02			
²²⁴ Yb	1565.9	6.39	5.71	5.76	6.18	0.43	0.12	1559.3	0.26	-0.04			
²²⁶ Yb	1568.2	6.39	5.69	5.75	6.18	0.39	0.15	1559.9	0.26	-0.06			
²²⁸ Yb	1569.3	6.43	5.72	5.77	6.22	0.41	0.12	1560.3	0.26	-0.07			
²³⁰ Yb	1570.2	6.46	5.73	5.79	6.25	0.41	0.11	1560.7	0.26	-0.09			
²³² Yb	1573.9	6.43	5.66	5.71	6.21	-0.24	-0.02	1560.7	0.25	-0.11			
²³⁴ Yb	1574.9	6.46	5.67	5.73	6.24	-0.24	-0.03	1559.5	0.23	-0.11			
²³⁶ Yb	1575.1	6.49	5.68	5.74	6.26	-0.22	-0.04						
²³⁸ Yb	1575.5	6.51	5.69	5.74	6.28	-0.21	-0.06						
²⁴⁰ Yb	1576.2	6.54	5.70	5.75	6.30	-0.19	-0.07						

Table 2: Same as Table-1 for Hf isotopes.

Nucleus	RMF (NL3)							FRDM			Expt.		
	BE(R)	r_n	r_p	r_{ch}	r_{rms}	β_2	β_4	BE(F)	β_2	β_4	BE(Ex)	r_{ch}	β_2
¹⁵² Hf	1198.8	5.06	5.09	5.15	5.07	-0.13	-0.02	1194.4	-0.15	-0.05			
¹⁵⁴ Hf	1223.1	5.07	5.08	5.14	5.07	-0.00	0.00	1219.9	0.01	0.00	1219.4		
¹⁵⁶ Hf	1243.7	5.11	5.09	5.15	5.10	0.07	0.01	1240.8	0.04	-0.01	1240.65		
¹⁵⁸ Hf	1264.5	5.16	5.12	5.18	5.14	0.14	0.03	1260.8	0.11	0.02	1261.0		
¹⁶⁰ Hf	1284.3	5.20	5.14	5.20	5.18	0.17	0.03	1280.8	0.15	0.02	1281.0		
¹⁶² Hf	1303.3	5.25	5.16	5.22	5.21	0.20	0.03	1300.2	0.18	0.01	1300.4		0.16
¹⁶⁴ Hf	1321.5	5.29	5.18	5.25	5.24	0.23	0.04	1319.0	0.21	0.01	1319.2		0.20
¹⁶⁶ Hf	1339.4	5.33	5.21	5.27	5.28	0.27	0.08	1337.3	0.23	0.00	1337.4		0.25
¹⁶⁸ Hf	1357.1	5.38	5.24	5.30	5.32	0.31	0.11	1355.2	0.25	-0.00	1355.0		0.28
¹⁷⁰ Hf	1374.0	5.42	5.26	5.32	5.35	0.32	0.10	1372.4	0.27	-0.01	1372.0	5.29	0.30
¹⁷² Hf	1390.1	5.46	5.28	5.34	5.38	0.33	0.08	1388.8	0.28	-0.02	1388.3	5.31	0.28
¹⁷⁴ Hf	1405.6	5.48	5.29	5.35	5.40	0.32	0.04	1404.6	0.29	-0.04	1403.9	5.32	0.29
¹⁷⁶ Hf	1420.5	5.51	5.29	5.35	5.42	0.31	0.01	1419.5	0.28	-0.06	1418.8	5.33	0.30
¹⁷⁸ Hf	1434.6	5.53	5.30	5.36	5.44	0.30	-0.01	1433.8	0.28	-0.08	1432.8	5.34	0.28
¹⁸⁰ Hf	1447.7	5.56	5.31	5.37	5.47	0.29	-0.04	1447.3	0.28	-0.10	1446.3	5.35	0.27
¹⁸² Hf	1460.0	5.59	5.33	5.39	5.49	0.28	-0.06	1459.8	0.27	-0.11	1458.7	5.35	
¹⁸⁴ Hf	1471.6	5.62	5.34	5.40	5.51	0.27	-0.07	1471.6	0.26	-0.13	1470.29		
¹⁸⁶ Hf	1481.8	5.64	5.34	5.4	5.53	0.24	-0.07	1482.9	0.25	-0.13	1481.3		
¹⁸⁸ Hf	1492.0	5.66	5.35	5.40	5.54	0.21	-0.07	1493.4	0.21	-0.11	1492.0		
¹⁹⁰ Hf	1501.8	5.68	5.35	5.41	5.56	0.18	-0.07	1503.2	0.16	-0.08			
¹⁹² Hf	1510.5	5.71	5.35	5.41	5.58	0.16	-0.06	1512.7	-0.18	-0.03			
¹⁹⁴ Hf	1519.0	5.72	5.35	5.41	5.59	-0.13	-0.03	1522.3	-0.12	-0.03			
¹⁹⁶ Hf	1528.9	5.74	5.36	5.42	5.60	-0.09	-0.04	1531.7	-0.08	-0.04			
¹⁹⁸ Hf	1537.8	5.77	5.36	5.41	5.62	0.00	0.00	1540.7	0.01	0.00			
²⁰⁰ Hf	1542.1	5.81	5.38	5.43	5.66	0.06	0.01	1546.0	0.02	0.00			
²⁰² Hf	1547.5	5.86	5.41	5.47	5.70	0.12	0.05	1550.1	0.05	0.02			
²⁰⁴ Hf	1553.4	5.90	5.43	5.49	5.74	0.16	0.08	1554.5	0.10	0.05			
²⁰⁶ Hf	1558.7	5.94	5.46	5.51	5.77	0.18	0.07	1559.2	0.13	0.06			
²⁰⁸ Hf	1564.0	5.98	5.48	5.54	5.81	0.20	0.06	1563.7	0.16	0.08			
²¹⁰ Hf	1568.7	6.02	5.50	5.56	5.85	0.22	0.05	1568.4	0.17	0.08			
²¹² Hf	1573.6	6.07	5.56	5.62	5.90	0.29	0.18	1572.8	0.20	0.07			
²¹⁴ Hf	1579.0	6.11	5.58	5.64	5.94	0.31	0.18	1577.0	0.22	0.07			
²¹⁶ Hf	1584.1	6.15	5.61	5.66	5.97	0.33	0.18	1580.8	0.22	0.05			
²¹⁸ Hf	1587.7	6.18	5.62	5.68	6.02	0.33	0.16	1584.4	0.23	0.04			
²²⁰ Hf	1591.2	6.21	5.64	5.69	6.03	0.33	0.13	1587.6	0.23	0.02			
²²² Hf	1594.7	6.24	5.66	5.71	6.06	0.33	0.10	1590.7	0.24	-0.00			
²²⁴ Hf	1597.8	6.27	5.67	5.72	6.09	0.33	0.07	1593.2	0.25	-0.02			
²²⁶ Hf	1600.8	6.30	5.67	5.73	6.11	0.32	0.03	1594.8	0.24	-0.03			
²²⁸ Hf	1603.3	6.32	5.68	5.73	6.13	0.31	-0.00	1596	0.23	-0.05			
²³⁰ Hf	1604.1	6.40	5.72	5.78	6.20	0.22	0.10	1597.5	0.24	-0.08			
²³² Hf	1607.8	6.37	5.7	5.76	6.17	0.29	-0.05	1598.8	0.24	-0.09			
²³⁴ Hf	1609.6	6.40	5.71	5.77	6.20	0.28	-0.06	1599.8	0.24	-0.11			
²³⁶ Hf	1611.4	6.44	5.72	5.77	6.23	0.26	-0.08	1599.4	0.22	-0.11			
²³⁸ Hf	1613.2	6.47	5.73	5.78	6.25	0.25	-0.09	1598.9	0.22	-0.12			
²⁴⁰ Hf	1614.5	6.49	5.74	5.80	6.27	0.25	-0.11	1596.4	0.17	-0.09			
²⁴² Hf	1614.7	6.51	5.75	5.80	6.30	0.23	-0.10						

Table 3: Same as Table-1 for W isotopes.

Nucleus	RMF (NL3)							FRDM			Expt.		
	BE(R)	r_n	r_p	r_{ch}	r_{rms}	β_2	β_4	BE(F)	β_2	β_4	BE(Ex)	r_{ch}	β_2
¹⁵⁴ W	1198.0	5.06	5.12	5.18	5.09	-0.11	-0.02	1192.8	-0.12	-0.04			
¹⁵⁶ W	1224.1	5.08	5.11	5.17	5.09	-0.01	0.0	1219.4	0.01	0.00			
¹⁵⁸ W	1245.6	5.12	5.12	5.19	5.12	-0.04	0.00	1241.7	0.02	0.00	1241.1		
¹⁶⁰ W	1267.1	5.16	5.15	5.21	5.16	0.11	0.01	1262.6	0.09	0.00	1262.9		
¹⁶² W	1287.9	5.20	5.17	5.23	5.19	0.15	0.01	1283.5	0.13	0.02	1283.7		
¹⁶⁴ W	1307.7	5.25	5.19	5.25	5.22	0.17	0.01	1303.9	0.16	0.01	1304.0		
¹⁶⁶ W	1326.6	5.29	5.21	5.27	5.25	0.20	0.02	1323.7	0.18	-0.00	1323.8		
¹⁶⁸ W	1345.4	5.35	5.25	5.31	5.31	0.28	0.02	1342.9	0.21	0.00	1343.0		0.23
¹⁷⁰ W	1364.5	5.39	5.28	5.34	5.34	0.32	0.12	1361.6	0.23	-0.01	1361.5		0.24
¹⁷² W	1382.6	5.43	5.30	5.36	5.37	0.33	0.11	1379.7	0.25	-0.00	1379.5		0.28
¹⁷⁴ W	1399.7	5.46	5.31	5.37	5.40	0.33	0.09	1397.1	0.27	-0.01	1396.7		0.25
¹⁷⁶ W	1416.1	5.49	5.32	5.38	5.42	0.33	0.06	1413.8	0.27	-0.03	1413.3		
¹⁷⁸ W	1431.9	5.51	5.33	5.39	5.44	0.31	0.02	1429.9	0.27	-0.05	1429.2		
¹⁸⁰ W	1447.0	5.54	5.33	5.39	5.45	0.29	-0.01	1445.4	0.26	-0.07	1444.6	5.35	0.25
¹⁸² W	1461.2	5.56	5.34	5.40	5.47	0.28	-0.04	1459.9	0.26	-0.08	1459.3	5.36	0.25
¹⁸⁴ W	1474.7	5.59	5.35	5.41	5.49	0.26	-0.06	1473.6	0.24	-0.10	1472.9	5.37	0.24
¹⁸⁶ W	1487.4	5.62	5.36	5.42	5.52	0.25	-0.08	1486.7	0.23	-0.11	1485.9	5.37	0.23
¹⁸⁸ W	1499.3	5.64	5.36	5.42	5.53	0.22	-0.08	1499.1	0.21	-0.11	1498.2		
¹⁹⁰ W	1510.9	5.65	5.37	5.43	5.54	0.20	-0.08	1510.8	0.17	-0.10	1509.9		
¹⁹² W	1521.8	5.68	5.37	5.43	5.56	0.17	-0.08	1522.28	0.16	-0.08	1521.41		
¹⁹⁴ W	1531.4	5.70	5.38	5.43	5.58	0.15	-0.07	1532.5	-0.17	-0.03			
¹⁹⁶ W	1540.8	5.72	5.38	5.43	5.59	0.11	-0.05	1543.3	-0.11	-0.03			
¹⁹⁸ W	1551.4	5.74	5.38	5.44	5.61	-0.08	-0.04	1553.8	-0.07	-0.04			
²⁰⁰ W	1561.6	5.76	5.38	5.44	5.62	0.00	0.00	1563.7	0.01	0.00			
²⁰² W	1566.2	5.80	5.40	5.46	5.66	0.03	0.00	1570.0	0.01	0.00			
²⁰⁴ W	1571.8	5.84	5.43	5.48	5.70	0.10	0.03	1575.1	0.04	0.01			
²⁰⁶ W	1577.9	5.89	5.45	5.51	5.73	0.14	0.06	1580.0	0.08	0.04			
²⁰⁸ W	1583.7	5.93	5.47	5.53	5.77	0.16	0.06	1585.2	0.11	0.05			
²¹⁰ W	1589.4	5.97	5.49	5.55	5.80	0.18	0.05	1590.4	0.14	0.06			
²¹² W	1594.3	6.02	5.55	5.61	5.86	0.26	0.14	1595.7	0.16	0.07			
²¹⁴ W	1600.9	6.06	5.58	5.64	5.90	0.29	0.16	1600.8	0.18	0.07			
²¹⁶ W	1606.9	6.10	5.60	5.66	5.94	0.31	0.16	1605.7	0.21	0.07			
²¹⁸ W	1612.7	6.14	5.62	5.68	5.97	0.32	0.16	1610.3	0.22	0.04			
²²⁰ W	1617.3	6.17	5.64	5.70	6.00	0.32	0.14	1614.6	0.22	0.03			
²²² W	1621.9	6.20	5.66	5.71	6.02	0.32	0.11	1618.6	0.23	0.00			
²²⁴ W	1626.2	6.23	5.68	5.73	6.05	0.33	0.09	1622.2	0.23	-0.01			
²²⁶ W	1629.9	6.26	5.69	5.75	6.08	0.33	0.07	1625.4	0.23	-0.03			
²²⁸ W	1633.5	6.30	5.70	5.76	6.11	0.33	0.04	1627.8	0.22	-0.04			
²³⁰ W	1636.3	6.32	5.72	5.77	6.14	0.33	0.02	1630.1	0.22	-0.06			
²³² W	1638.8	6.35	5.73	5.79	6.16	0.32	-0.00	1632.4	0.22	-0.07			
²³⁴ W	1641.3	6.37	5.74	5.80	6.18	0.30	-0.03	1634.5	0.22	-0.08			
²³⁶ W	1643.3	6.40	5.75	5.80	6.20	0.28	-0.05	1636.3	0.22	-0.10			
²³⁸ W	1645.5	6.42	5.75	5.80	6.22	0.26	-0.08	1636.9	0.21	-0.11			
²⁴⁰ W	1648.1	6.45	5.76	5.81	6.24	0.25	-0.10	1636.9	0.19	-0.10			
²⁴² W	1650.5	6.47	5.77	5.83	6.27	0.24	-0.12	1635.9	0.16	-0.09			
²⁴⁴ W	1651.1	6.50	5.77	5.83	6.29	0.22	-0.11	1636.2	0.16	-0.10			

Table 4: Same as Table-1 for Os isotopes.

Nucleus	RMF (NL3)							FRDM			Expt.		
	BE(R)	r_n	r_p	r_{ch}	r_{rms}	β_2	β_4	BE(F)	β_2	β_4	BE(Ex)	r_{ch}	β_2
¹⁵⁶ Os	1195.9	5.06	5.15	5.21	5.10	-0.08	-0.02						
¹⁵⁸ Os	1223.8	5.08	5.14	5.21	5.11	-0.00	0.00						
¹⁶⁰ Os	1246.4	5.12	5.16	5.22	5.14	-0.00	0.00	1241.0	0.01				
¹⁶² Os	1287.9	5.20	5.17	5.23	5.19	0.15	0.00	1262.8	0.05	-0.01	1262.6		
¹⁶⁴ Os	1307.7	5.25	5.19	5.25	5.22	0.17	0.00	1284.5	0.11	-0.00	1284.7		
¹⁶⁶ Os	1310.3	5.24	5.21	5.27	5.23	0.13	-0.00	1305.8	0.13	-0.00	1305.8		
¹⁶⁸ Os	1330.0	5.28	5.23	5.29	5.26	0.16	0.00	1326.6	0.16	-0.01	1326.5		
¹⁷⁰ Os	1349.3	5.35	5.28	5.34	5.32	0.27	0.10	1346.7	0.17	-0.01	1346.6		
¹⁷² Os	1382.5	5.43	5.30	5.36	5.37	0.33	0.11	1366.3	0.19	-0.01	1366.05		0.23
¹⁷⁴ Os	1388.5	5.43	5.33	5.39	5.39	0.32	0.10	1385.3	0.23	-0.01	1384.9		0.27
¹⁷⁶ Os	1416.9	5.49	5.32	5.38	5.42	0.33	0.08	1403.6	0.25	-0.01	1403.2		
¹⁷⁸ Os	1424.3	5.50	5.36	5.42	5.44	0.33	0.06	1421.3	0.25	-0.03	1420.8		
¹⁸⁰ Os	1441.4	5.52	5.37	5.43	5.46	0.32	0.03	1438.5	0.24	-0.05	1437.7		0.23
¹⁸² Os	1461.2	5.56	5.34	5.40	5.47	0.28	0.00	1454.9	0.24	-0.06	1454.1		0.23
¹⁸⁴ Os	1472.3	5.57	5.38	5.44	5.49	0.29	-0.03	1470.7	0.23	-0.07	1469.9	5.38	0.21
¹⁸⁶ Os	1487.4	5.62	5.36	5.42	5.52	0.25	-0.05	1485.4	0.22	-0.08	1484.8	5.39	0.20
¹⁸⁸ Os	1500.0	5.62	5.39	5.45	5.53	0.24	-0.07	1499.3	0.19	-0.09	1499.1	5.40	0.19
¹⁹⁰ Os	1512.9	5.63	5.38	5.44	5.53	0.20	-0.07	1512.8	0.16	-0.08	1512.8	5.41	0.18
¹⁹² Os	1526.1	5.65	5.38	5.44	5.54	0.18	-0.07	1526.3	0.16	-0.08	1526.1	5.41	0.17
¹⁹⁴ Os	1531.4	5.70	5.37	5.43	5.58	0.15	-0.07	1539.0	0.15	-0.08	1538.8		
¹⁹⁶ Os	1549.6	5.69	5.39	5.45	5.57	0.12	-0.06	1550.5	-0.16	-0.03	1550.8		
¹⁹⁸ Os	1551.4	5.74	5.38	5.44	5.61	-0.10	-0.04	1562.6	-0.10	-0.03			
²⁰⁰ Os	1572.6	5.73	5.40	5.46	5.61	-0.06	-0.03	1574.1	-0.06	-0.04			
²⁰² Os	1584.1	5.76	5.40	5.46	5.63	0.00	-0.00	1584.9	0.01	0.00			
²⁰⁴ Os	1589.6	5.80	5.42	5.48	5.66	0.00	-0.00	1592.0	0.01	0.00			
²⁰⁶ Os	1594.8	5.83	5.44	5.50	5.69	0.07	0.01	1598.0	0.03	0.01			
²⁰⁸ Os	1583.7	5.93	5.47	5.53	5.77	0.16	0.04	1603.7	0.05	0.02			
²¹⁰ Os	1607.4	5.91	5.49	5.55	5.76	0.14	0.05	1609.5	0.10	0.04			
²¹² Os	1613.4	5.95	5.51	5.57	5.80	0.16	0.05	1615.4	0.12	0.05			
²¹⁴ Os	1600.9	6.06	5.58	5.64	5.90	0.29	0.13	1621.1	0.15	0.05			
²¹⁶ Os	1625.6	6.05	5.60	5.65	5.89	0.27	0.15	1627.0	0.17	0.06			
²¹⁸ Os	1632.2	6.09	5.63	5.68	5.93	0.30	0.15	1632.5	0.20	0.06			
²²⁰ Os	1638.9	6.13	5.65	5.71	5.97	0.32	0.15	1637.9	0.21	0.05			
²²² Os	1644.6	6.16	5.67	5.73	6.00	0.33	0.13	1642.9	0.21	0.03			
²²⁴ Os	1650.0	6.19	5.69	5.75	6.02	0.33	0.10	1647.7	0.22	0.02			
²²⁶ Os	1655.3	6.22	5.71	5.77	6.06	0.34	0.09	1652.0	0.22	0.00			
²²⁸ Os	1659.7	6.26	5.72	5.78	6.09	0.34	0.02	1656.0	0.23	-0.02			
²³⁰ Os	1663.8	6.29	5.74	5.79	6.09	0.34	0.04	1659.2	0.22	-0.03			
²³² Os	1667.6	6.32	5.76	5.81	6.14	0.33	0.02	1662.2	0.21	-0.05			
²³⁴ Os	1670.6	6.34	5.77	5.82	6.16	0.32	-0.00	1665.1	0.20	-0.06			
²³⁶ Os	1673.5	6.36	5.77	5.83	6.18	0.31	-0.02	1668.0	0.20	-0.07			
²³⁸ Os	1675.8	6.39	5.78	5.83	6.20	0.29	-0.05	1670.5	0.21	-0.09			
²⁴⁰ Os	1678.4	6.42	5.78	5.84	6.22	0.27	-0.07	1671.7	0.18	-0.09			
²⁴² Os	1681.1	6.44	5.79	5.85	6.24	0.26	-0.09	1671.9	0.16	-0.08			
²⁴⁴ Os	1683.8	6.47	5.80	5.86	6.27	0.25	-0.11	1672.6	0.16	-0.07			
²⁴⁶ Os	1684.5	6.49	5.81	5.86	6.29	0.23	-0.10	1671.2	0.11	-0.03			

Table 5: Same as Table-1 for Pt isotopes.

Nucleus	RMF (NL3)							FRDM			Expt.		
	BE(R)	r_n	r_p	r_{ch}	r_{rms}	β_2	β_4	BE(F)	β_2	β_4	BE(Ex)	r_{ch}	β_2
¹⁵⁸ Pt	1192.2	5.06	5.18	5.24	5.12	-0.00	0.00						
¹⁶⁰ Pt	1222.1	5.09	5.18	5.24	5.13	-0.002	0.00						
¹⁶² Pt	1246.0	5.13	5.19	5.25	5.16	-0.00	0.00						
¹⁶⁴ Pt	1268.2	5.16	5.20	5.27	5.18	-0.03	0.00						
¹⁶⁶ Pt	1290.3	5.20	5.22	5.28	5.21	0.07	0.00	1283.8	-0.07	-0.01	1283.7		
¹⁶⁸ Pt	1310.0	5.24	5.24	5.30	5.24	0.08	-0.00	1305.6	-0.10	-0.01	1306.0		
¹⁷⁰ Pt	1332.0	5.28	5.25	5.31	5.26	0.09	-0.01	1327.2	0.11	-0.00	1327.4		
¹⁷² Pt	1351.3	5.35	5.30	5.36	5.33	0.25	0.09	1348.2	0.13	-0.01	1348.3		
¹⁷⁴ Pt	1372.2	5.40	5.33	5.39	5.33	0.29	0.11	1368.7	0.15	-0.01	1368.7		
¹⁷⁶ Pt	1392.3	5.44	5.36	5.41	5.40	0.31	0.10	1388.5	0.17	-0.01	1388.5		0.19
¹⁷⁸ Pt	1411.7	5.47	5.37	5.43	5.43	0.32	0.08	1407.9	0.25	0.01	1407.7	5.37	
¹⁸⁰ Pt	1430.6	5.50	5.39	5.45	5.45	0.32	0.05	1426.4	0.27	-0.01	1426.2	5.39	0.26
¹⁸² Pt	1448.8	5.53	5.40	5.46	5.48	0.32	0.03	1444.4	0.26	-0.03	1444.1	5.40	
¹⁸⁴ Pt	1465.7	5.56	5.41	5.47	5.50	0.31	0.01	1461.9	0.25	-0.04	1461.4	5.40	0.22
¹⁸⁶ Pt	1481.6	5.58	5.42	5.48	5.51	0.30	-0.01	1478.5	0.24	-0.06	1478.1	5.40	0.20
¹⁸⁸ Pt	1496.2	5.61	5.42	5.48	5.53	0.28	-0.03	1493.5	-0.16	-0.01	1494.2	5.41	0.19
¹⁹⁰ Pt	1510.0	5.63	5.42	5.48	5.54	0.25	-0.05	1509.1	-0.16	-0.02	1509.9	5.41	0.15
¹⁹² Pt	1524.3	5.62	5.40	5.46	5.53	0.18	-0.06	1524.2	-0.16	-0.03	1525.0	5.42	0.15
¹⁹⁴ Pt	1538.9	5.64	5.40	5.45	5.54	0.14	-0.06	1539.0	-0.15	-0.03	1539.6	5.42	0.14
¹⁹⁶ Pt	1552.8	5.66	5.40	5.46	5.55	-0.13	-0.03	1553.2	-0.14	-0.03	1553.6	5.43	0.13
¹⁹⁸ Pt	1566.3	5.68	5.40	5.46	5.46	-0.11	-0.02	1566.8	-0.14	-0.03	1567.0	5.44	0.11
²⁰⁰ Pt	1579.6	5.70	5.41	5.47	5.59	-0.08	-0.03	1580.0	-0.09	-0.03	1579.9		
²⁰² Pt	1592.5	5.72	5.42	5.47	5.61	-0.00	0.00	1592.5	-0.06	-0.04			
²⁰⁴ Pt	1605.3	5.75	5.42	5.48	5.63	0.00	0.00	1604.1	0.01	0.00			
²⁰⁶ Pt	1611.6	5.79	5.44	5.5	5.66	0.00	0.00	1612.1	0.01	0.00			
²⁰⁸ Pt	1617.1	5.83	5.46	5.52	5.69	-0.04	0.01	1618.9	0.03	0.00			
²¹⁰ Pt	1615.2	6.00	5.65	5.70	5.87	0.09	0.12	1625.5	0.05	0.01			
²¹² Pt	1623.7	6.04	5.67	5.73	5.91	0.14	0.12	1631.9	0.08	0.03			
²¹⁴ Pt	1635.8	5.94	5.53	5.58	5.79	0.13	0.05	1638.4	0.11	0.04			
²¹⁶ Pt	1641.7	6.00	5.58	5.64	5.85	0.22	0.12	1644.9	0.13	0.05			
²¹⁸ Pt	1649.0	6.04	5.61	5.67	5.89	0.25	0.14	1651.2	0.16	0.07			
²²⁰ Pt	1656.1	6.08	5.64	5.70	5.93	0.29	0.14	1657.4	0.19	0.07			
²²² Pt	1663.3	6.12	5.67	5.73	5.97	0.31	0.14	1663.4	0.20	0.06			
²²⁴ Pt	1669.8	6.15	5.69	5.75	6.00	0.31	0.11	1669.2	0.21	0.05			
²²⁶ Pt	1676.1	6.18	5.71	5.77	6.02	0.32	0.09	1674.6	0.22	0.03			
²²⁸ Pt	1682.2	6.21	5.73	5.78	6.05	0.32	0.07	1679.7	0.22	0.02			
²³⁰ Pt	1687.0	6.25	5.74	5.80	6.08	0.32	0.05	1684.3	0.23	-0.00			
²³² Pt	1691.7	6.28	5.76	5.81	6.11	0.33	0.02	1688.2	0.21	-0.02			
²³⁴ Pt	1696.3	6.31	5.78	5.83	6.14	0.33	0.00	1691.8	0.19	-0.03			
²³⁶ Pt	1700.4	6.33	5.79	5.84	6.16	0.31	-0.01	1695.2	0.18	-0.04			
²³⁸ Pt	1704.3	6.35	5.80	5.86	6.18	0.30	-0.03	1698.8	0.18	-0.05			
²⁴⁰ Pt	1707.3	6.38	5.81	5.87	6.20	0.29	-0.05	1702.1	0.19	-0.08			
²⁴² Pt	1710.2	6.41	5.82	5.88	6.23	0.28	-0.07	1704.1	0.17	-0.09			
²⁴⁴ Pt	1713.2	6.44	5.83	5.89	6.25	0.27	-0.08	1705.3	0.16	-0.06			
²⁴⁶ Pt	1716.2	6.47	5.84	5.90	6.28	0.26	-0.10	1705.7	0.10	-0.03			
²⁴⁸ Pt	1716.7	6.46	5.77	5.83	6.25	-0.15	-0.08	1706.8	0.09	-0.01			

Table 6: Same as Table-1 for Hg isotopes.

Nucleus	RMF (NL3)							FRDM			Expt.		
	BE(R)	r_n	r_p	r_{ch}	r_{rms}	β_2	β_4	BE(F)	β_2	β_4	BE(Ex)	r_{ch}	β_2
¹⁶⁰ Hg	1187.3	5.07	5.22	5.28	5.15	-0.00	0.00						
¹⁶² Hg	1218.7	5.10	5.22	5.28	5.16	-0.00	0.00						
¹⁶⁴ Hg	1243.9	5.13	5.22	5.29	5.18	-0.00	0.00						
¹⁶⁶ Hg	1267.0	5.17	5.24	5.30	5.20	-0.00	0.00						
¹⁶⁸ Hg	1289.7	5.21	5.25	5.31	5.23	-0.01	0.00						
¹⁷⁰ Hg	1312.2	5.24	5.27	5.33	5.25	-0.00	0.00	1304.7	-0.08	-0.01			
¹⁷² Hg	1334.0	5.27	5.28	5.34	5.28	-0.00	0.00	1326.9	-0.10	-0.02	1326.8		
¹⁷⁴ Hg	1354.6	5.31	5.29	5.35	5.3	0.00	0.00	1348.5	-0.11	-0.03	1348.5		
¹⁷⁶ Hg	1373.3	5.40	5.36	5.42	5.38	0.27	0.11	1369.6	-0.11	-0.03	1369.7		
¹⁷⁸ Hg	1394.3	5.44	5.38	5.44	5.41	0.30	0.10	1390.1	-0.11	-0.03	1390.4		
¹⁸⁰ Hg	1414.7	5.47	5.40	5.46	5.44	0.31	0.08	1410.2	-0.12	-0.03	1410.5		
¹⁸² Hg	1434.5	5.51	5.41	5.47	5.47	0.31	0.06	1429.8	-0.12	-0.02	1430.0	5.38	
¹⁸⁴ Hg	1453.7	5.54	5.43	5.48	5.49	0.31	0.03	1448.9	-0.13	-0.02	1448.9	5.39	0.16
¹⁸⁶ Hg	1471.6	5.56	5.44	5.49	5.51	0.31	0.01	1467.3	-0.13	-0.03	1467.2	5.40	0.13
¹⁸⁸ Hg	1488.4	5.59	5.44	5.50	5.53	0.30	-0.01	1485.1	-0.13	-0.03	1485.0	5.41	
¹⁹⁰ Hg	1504.1	5.61	5.45	5.51	5.55	0.28	-0.03	1502.3	-0.13	-0.03	1502.3	5.42	
¹⁹² Hg	1520.1	5.59	5.40	5.46	5.51	-0.15	-0.02	1519	-0.13	-0.03	1519.1	5.42	
¹⁹⁴ Hg	1536.3	5.61	5.41	5.46	5.53	-0.14	-0.03	1535.2	-0.13	-0.04	1535.4	5.43	
¹⁹⁶ Hg	1552.1	5.63	5.41	5.47	5.55	-0.14	-0.03	1551.1	-0.12	-0.03	1551.2	5.44	0.12
¹⁹⁸ Hg	1567.4	5.66	5.42	5.48	5.56	-0.12	-0.02	1566.3	-0.12	-0.03	1566.5	5.45	0.11
²⁰⁰ Hg	1582.1	5.68	5.42	5.48	5.58	-0.09	-0.02	1581.0	-0.11	-0.03	1581.2	5.46	0.10
²⁰² Hg	1596.4	5.70	5.43	5.49	5.59	-0.00	0.00	1595.1	-0.09	-0.04	1595.2	5.46	0.08
²⁰⁴ Hg	1610.8	5.72	5.44	5.49	5.59	0.00	0.00	1608.6	-0.06	-0.04	1608.7	5.47	0.07
²⁰⁶ Hg	1624.3	5.75	5.44	5.50	5.63	0.00	0.00	1621.3	-0.01	0.00	1621.0	5.48	
²⁰⁸ Hg	1631.6	5.79	5.46	5.52	5.67	0.00	0.00	1630.3	-0.01	0.01	1629.3		
²¹⁰ Hg	1637.5	5.82	5.48	5.54	5.70	-0.00	0.00	1638.0	-0.03	-0.01	1637.6		
²¹² Hg	1644.0	5.86	5.51	5.56	5.73	-0.05	0.00	1645.4	-0.04	-0.01			
²¹⁴ Hg	1650.4	5.89	5.53	5.59	5.76	-0.06	-0.00	1652.7	-0.05	-0.01			
²¹⁶ Hg	1652.1	6.09	5.74	5.80	5.96	0.12	0.15	1659.5	-0.08	-0.01			
²¹⁸ Hg	1663.2	5.98	5.59	5.65	5.84	0.19	0.12	1666.3	-0.09	-0.01			
²²⁰ Hg	1670.8	6.03	5.62	5.68	5.88	0.23	0.14	1673.3	0.16	0.08			
²²² Hg	1678.6	6.07	5.66	5.71	5.92	0.27	0.14	1680.3	0.19	0.08			
²²⁴ Hg	1686.2	6.11	5.68	5.74	5.96	0.29	0.13	1687.0	0.20	0.06			
²²⁶ Hg	1693.2	6.14	5.70	5.76	5.99	0.30	0.11	1693.5	0.21	0.06			
²²⁸ Hg	1700.0	6.17	5.72	5.78	6.02	0.30	0.09	1699.6	0.22	0.04			
²³⁰ Hg	1706.4	6.20	5.74	5.79	6.04	0.31	0.07	1705.4	0.22	0.03			
²³² Hg	1711.8	6.23	5.76	5.81	6.07	0.31	0.05	1710.7	0.23	0.01			
²³⁴ Hg	1717.3	6.27	5.78	5.84	6.11	0.32	0.02	1715.2	0.22	-0.01			
²³⁶ Hg	1722.8	6.30	5.80	5.86	6.14	0.32	-0.10	1719.5	0.20	-0.02			
²³⁸ Hg	1727.8	6.32	5.82	5.87	6.16	0.31	-0.03	1723.7	0.19	-0.04			
²⁴⁰ Hg	1732.4	6.35	5.83	5.88	6.18	0.30	-0.04	1728.0	0.19	-0.05			
²⁴² Hg	1736.4	6.37	5.84	5.90	6.20	0.29	-0.06	1731.7	0.20	-0.07			
²⁴⁴ Hg	1739.9	6.40	5.85	5.91	6.23	0.28	-0.08	1732.5	-0.06	0.00			
²⁴⁶ Hg	1743.3	6.43	5.86	5.92	6.25	0.27	-0.09	1736.0	-0.07	0.00			
²⁴⁸ Hg	1744.5	6.42	5.79	5.85	6.23	-0.18	-0.04	1739.5	-0.09	-0.01			
²⁵⁰ Hg	1748.5	6.45	5.79	5.85	6.24	-0.16	-0.06	1742.4	-0.10	0.00			

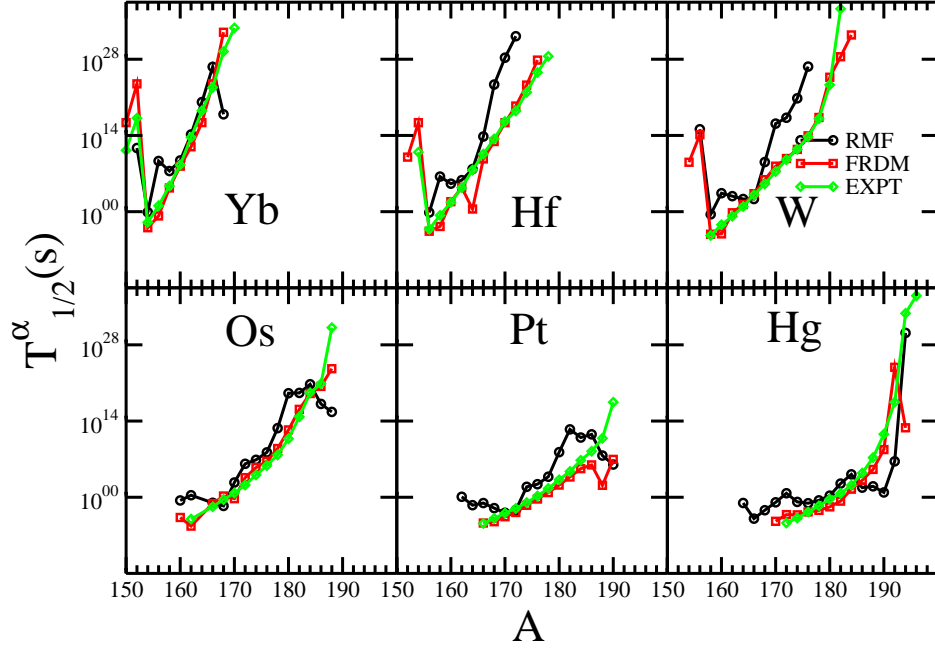


Figure 8: (Color online) The $T_{1/2}^{\alpha}$ obtained from RMF(NL3)(circle) are compared with FRDM(square) and experimental(diamond) results in $Z = 70 - 80$ region.

nuclei prefer β decay rather than going to α decay mode. Further we concluded that the RMF-BCS theory provides a reasonably good description for all the considered isotopes.

6 Acknowledgment

The author S. Mahapatro thanks Institute of Physics, Bhubaneswar, India for providing library and computer facilities for these calculations.

References

- [1] I. Hamamoto, *Phys. Rev. C* **85**, 064329 (2012).

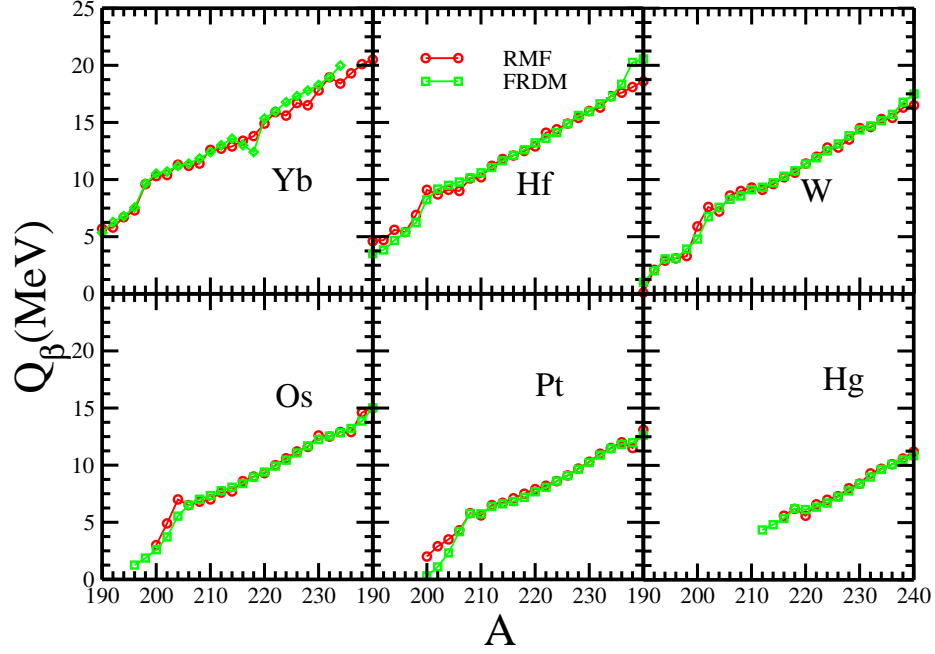


Figure 9: (Color online) The Q_β energy obtained from RMF(NL3)(circle) are compared with the FRDM(square) data for different isotopes in $Z = 70 - 80$ region.

- [2] T. Boumann, A. Spyrou and M. Theonnessen, *Rep. Prog. Phys.* **75** 036301 (2012).
- [3] P. J. Nolan and P. J. Twin, *Annu. Rev. Nucl. Part. Sci.* **38**, 533 (1988).
- [4] S. Åberg, H. Flocard and W. Nazarewicz, *Annu. Rev. Nucl. Part. Sci.* **40**, 439 (1990).
- [5] C. Baktash, B. Haas and W. Nazarewicz, *Annu. Rev. Nucl. Part. Sci.* **45**, 485 (1995).
- [6] C. Baktash, *Prog. Part. Nucl. Phys.* **38**, 291 (1997).
- [7] P. J. Twin, B. M. Nyakó, A. H. Nelson, J. Simpson, M. A. Bentley, H. W. Cranmer-Gordon, P. D. Forsyth, D. Howe, A. R. Mokhtar, J. D. Morrison, J. F. Sharpey-Schafer, G. Slethen, *Phys. Rev. Lett.* **57**, 811 (1986).
- [8] P. Quentin and H. Flocard, *Annu. Rev. Nucl. Part. Sci.* **28**, 23 (1978).

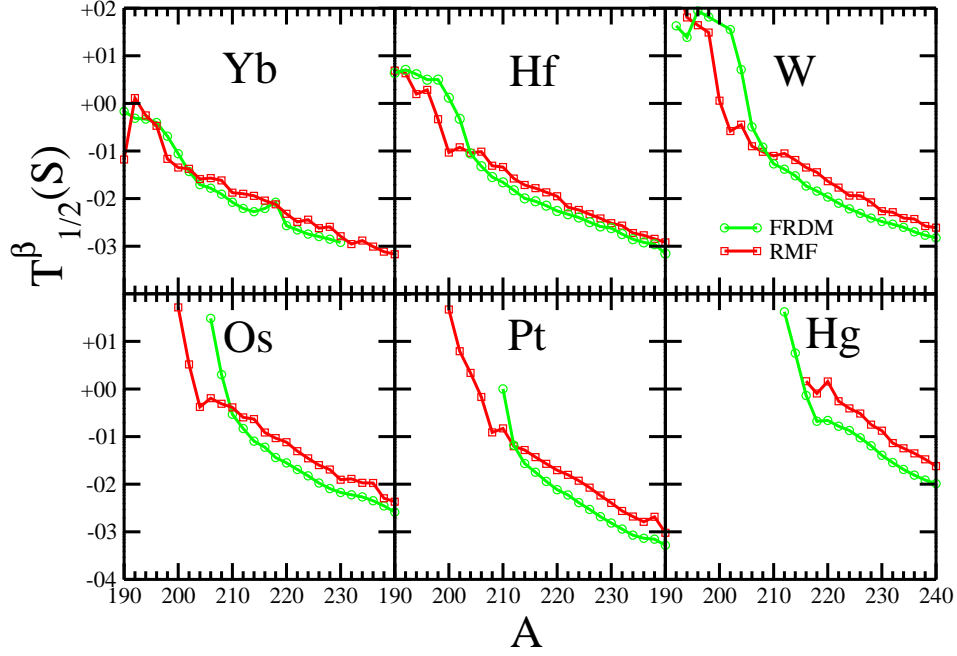


Figure 10: (Color online) The $T_{1/2}^{\beta}$ obtained from RMF(NL3)(circle) are compared with FRDM(square) data in $Z = 70 - 80$ region.

- [9] M. Baranger and K. Kumar, *Nucl. Phys. A* **110**, 410 (1968).
- [10] G. D. Alkhazov et al., *Nucl. Phys. A* **504**, 549 (1989) .
- [11] C. Thibault et al., *Nucl. Phys. A* **367**, 1 (1981).
- [12] I. Y. Lee et al., *Phys. Rev. Lett.* **39**, 682 (1974).
- [13] S. K. Patra and P. K. Panda, *Phys. Rev. C* **47**,1514 (1993).
- [14] M. M. Sharma and P. Ring, *Phys. Rev. C* **46**, 1715 (1992).
- [15] B. Kumar, S. K. Singh and S. K. Patra, *Int. Jour. of Mod. Phys. E* **24**, 1550017 (2015).
- [16] E. Bashandy, M. S. El-Nesr, *Z. Naturforsch. A* **29**, 1125 (2014).
- [17] P. R. John et al., *Phys. Rev. C* **90**,021301(R) (2014).

- [18] G.A. Lalazissis, S. Raman, and P. Ring, *Atomic Data and Nuclear Data Tables* **71**, 1 (1999).
- [19] P. Dabkiewicz et al., *Phys. Lett. B* **82**, 199 (1979).
- [20] M. Girod and J. P. Delaroche, *Phys. Rev. C* **45**,1420 (1993).
- [21] Y. K. Gambhir, P. Ring and A. Thimet, *Ann. Phys. (NY)* **198**, 132 (1990).
- [22] S. K. Patra and C. R. Praharaaj, *Phys. Rev. C* **44**, 2552 (1991).
- [23] J. D. Walecka, *Ann. Phys. (NY)* **83**, 491 (1974).
- [24] B. D. Serot and J. D. Walecka, *Adv. Nucl. Phys.* **16**, 1 (1986).
- [25] C. J. Horowitz and B. D. Serot, *Nucl. Phys. A* **368**, 503 (1981).
- [26] J. Boguta and A. R. Bodmer, *Nucl. Phys. A* **292**, 413 (1977).
- [27] C. E. Price and G. E. Walker, *Phys. Rev. C* **36**, 354 (1987).
- [28] T. Niksic et al., *Prog. Part. Nucl. Phys.* **66**, 519 (2011).
- [29] G. A. Lalazissis, J. König and P. Ring, *Phys. Rev. C* **55**, 1 (1997).
- [30] S. K. Patra, *Phys. Rev. C* **48**, 1449 (1993).
- [31] M. A. Preston and R. K. Bhaduri, *Structure of Nucleus, Addison-Wesley Publishing Company, 1982*, Ch. 8, page 309.
- [32] D. G. Madland and J. R. Nix, *Nucl. Phys. A* **476**, 1 (1981).
- [33] P. Möller and J.R. Nix, *At. Data and Nucl. Data Tables* **39**, 213 (1988).
- [34] G. A. Lalazissis, M. M. Sharma, P. Ring, *Nucl. Phys. A* **597**, 35 (1996).
- [35] K. Pomorski et al., *Nucl. Phys. A* **624**, 349 (1997).
- [36] P. Ring, *Prog. Part. Nucl. Phys.* **37**, 193 (1996).
- [37] J. Dobaczewski, H. Flocard and J. Treiner, *Nucl. Phys. A* **422**, 103 (1984).
- [38] J. Dobaczewski, W. Nazarewicz, T.R. Werner, J.F. Berger, C.R. Chinn and J. Decharge, *Phys. Rev. C* **53**, 2809 (1996).
- [39] J. Meng et al., *Prog. Part. Nucl. Phys.* **57**, 470 (2006).
- [40] J. Meng, *Nucl. Phys. A* **635**, 3 (1998).
- [41] M. Stoitsov, P. Ring, D. Vretenar and G. A. Lalazissis, *Phys. Rev. C* **58**, 2086 (1998).
- [42] T. Nikšić, D. Vretenar, P.Ring and G. A. Lalazissis, *Phys. Rev. C* **65**, 054320 (2002).

- [43] D. Vretenar, A. V. Afanasjev, G. A. Lalazissis and P. Ring, *Phys. Rep.* **409**, 101 (2005).
- [44] P. Möller, J. R. Nix and K. -L. Kratz, *Atomic and Nucl. Data Tables* **66**, 131 (1997).
- [45] M. Wang, G. Audi, A. H. Wapstra, F. G. Kondev, M. Mac-Cormick, X. Xu and P. Pfeiffer, *Chin. Phys. C* **36**, 1603 (2012).
- [46] S. K. Patra, M. Del Etal, M. Centelles, and X. Vinas, *Phys. Rev. C* **63**, 024311 (2001).
- [47] T. R. Werner, J. A. Sheikh, W. Nazarewicz, M. R. Strayer, A. S. Umar, and M. Mish, *Phys. Lett. B* **335**, 259 (1994).
- [48] T. R. Werner, J. A. Sheikh, M. Mish, W. Nazarewicz, J. Rikovska, K. Heeger, A. S. Umar, and M. R. Strayer, *Nucl. Phys. A* **597**, 327 (1996).
- [49] G. A. Lalazissis, D. Vretener, P. Ring, M. Stoitsor and L. M. Robledo, *Phys. Rev. C* **60**, 014310 (1999).
- [50] G. A. Lalazissis, D. Vretenar, and P. Ring, *Nucl. Phys. A* **650**, 133 (1999).
- [51] P. Arumugam, B. K. Sharma, S. K. Patra and Raj Kumar Gupta, *Phys. Rev. C* **71**, 064308 (2005).
- [52] B. Kumar, S. K. Singh, S. K. Biswal, S. K. Patra, *Phys. Rev. C* **92**, 054314 (2015).
- [53] Y. K. Gambhir, *Nucl. Phys. A* **570**, 101 (1994).
- [54] P. Möller, J. R. Nix, W. D. Myers and W. J. Swiatecki, *Atomic and Nucl. Data Tables* **59**, 185 (1995).
- [55] S. Raman, C. W. Jr. Nestor and P. Tikkanen, *Atomic and Nucl. Data Tables* **78**, 1 (2001).
- [56] I. Angeli and K. P. Marinova, *Atomic and Nucl. Data Tables* **99**, 69 (2013).
- [57] S. K. Patra and C. R. Praharaaj, *J. Phys. G* **23**, 939 (1997).
- [58] V. E. Viola, Jr. and G. T. Seaborg, *J. Inorg. Nucl. Chem.* **28**, 741 (1966).
- [59] A. Sobiczewski, Z. Patyk, and S. C. Cwiok, *Phys. Lett B* **224**, 1 (1989).
- [60] E. O. Fiset and J. R. Nix, *Nucl. Phys. A* **193**, 647 (1972).
- [61] S. K. Patra, M. Del Estal, M. Centelles and X. Viñas, *Phys. Rev. C* **63**, 024311 (2001).